Am J Physiol Regul Integr Comp Physiol 318: R360–R368, 2020.
First published December 18, 2019; doi:10.1152/ajpregu.00304.2019.

RESEARCH ARTICLE | *Physical Activity and Inactivity*

Synergist ablation-induced hypertrophy occurs more rapidly in the plantaris than soleus muscle in rats due to different molecular mechanisms

Michael D. Roberts,[1,2] Christopher B. Mobley,[3,4] Christopher G. Vann,[1] Cody T. Haun,[5] Brad J. Schoenfeld,[6] Kaelin C. Young,[1,2] and Andreas N. Kavazis[1]

[1]*School of Kinesiology, Auburn University, Auburn, Alabama;* [2]*Department of Cell Biology and Physiology, Edward Via College of Veterinary Medicine, Auburn, Alabama;* [3]*Department of Physiology, College of Medicine, University of Kentucky, Lexington, Kentucky;* [4]*Center for Muscle Biology, University of Kentucky, Lexington, Kentucky;* [5]*Department of Exercise Science, LaGrange College, LaGrange, Georgia; and* [6]*Department of Health Sciences, City University of New York Lehman College, Bronx, New York*

Submitted 16 October 2019; accepted in final form 9 December 2019

Roberts MD, Mobley CB, Vann CG, Haun CT, Schoenfeld BJ, Young KC, Kavazis AN. Synergist ablation-induced hypertrophy occurs more rapidly in the plantaris than soleus muscle in rats due to different molecular mechanisms. *Am J Physiol Regul Integr Comp Physiol* 318: R360–R368, 2020. First published December 18, 2019; doi:10.1152/ajpregu.00304.2019.—We examined molecular mechanisms that were altered during rapid soleus (type I fiber-dominant) and plantaris (type II fiber-dominant) hypertrophy in rats. Twelve Wistar rats (3.5 mo old; 6 female, 6 male) were subjected to surgical right-leg soleus and plantaris dual overload [synergist ablation (SA)], and sham surgeries were performed on left legs (CTL). At 14 days after surgery, the muscles were dissected. Plantaris mass was 27% greater in the SA than CTL leg ($P < 0.001$), soleus mass was 13% greater in the SA than CTL leg ($P < 0.001$), and plantaris mass was higher than soleus mass in the SA leg ($P = 0.001$). Plantaris total RNA concentrations and estimated total RNA levels (suggestive of ribosome density) were 19% and 47% greater in the SA than CTL leg ($P < 0.05$), protein synthesis levels were 64% greater in the SA than CTL leg ($P = 0.038$), and satellite cell number per fiber was 60% greater in the SA than CTL leg ($P = 0.003$); no differences in these metrics were observed between soleus SA and CTL legs. Plantaris, as well as soleus, 20S proteasome activity was lower in the SA than CTL leg ($P < 0.05$), although the degree of downregulation was greater in the plantaris than soleus muscle (−63% vs. −20%, $P = 0.001$). These data suggest that early-phase plantaris hypertrophy occurs more rapidly than soleus hypertrophy, which coincided with greater increases in ribosome biogenesis, protein synthesis, and satellite cell density, as well as greater decrements in 20S proteasome activity, in the plantaris muscle.

hypertrophy; rats; ribosomes; satellite cells; synergist ablation

INTRODUCTION

Molecular mechanisms that regulate skeletal muscle hypertrophy in response to overload include increases in muscle protein synthesis (MPS), decreases in muscle protein breakdown, an enhancement of satellite cell proliferation, and myonuclear accretion from a subset of satellite cells (33). Pioneered by Fred Goldberg's laboratory (11), the surgical synergist ablation (SA) model has been commonly used to examine mechanisms associated with rapid skeletal muscle hypertrophy in rodents. While various iterations of this surgery exist (31), a common procedure involves removal of a portion of the gastrocnemius muscle and soleus muscle to overload the plantaris muscle. A recent review on the topic indicated that the plantaris muscle undergoes a linear growth phase 1–15 days following surgery, with a plateau at 15–30 days postsurgery (35). Critically, muscle growth within the first 3–5 days has been attributed (in part) to edema and inflammation, whereas growth thereafter seems to reflect "true" hypertrophy, in the sense that these factors typically subside (35).

The dual-overload model involves removal of a portion of the gastrocnemius muscle while the plantaris and soleus muscles are left intact; this model has been used to induce hypertrophic adaptations in the plantaris and soleus muscles (4, 7, 14, 22, 39). While this model causes a less robust increase in postsurgical plantaris mass, a major strength of this model is that it allows researchers to examine molecular phenomena in a type I fiber-prominent (soleus, >90% type I fibers), as well as a type II fiber-prominent (plantaris, >90% type II fibers), muscle (2, 30).

It is generally accepted that both type I and type II fibers hypertrophy in response to an overload stimulus. However, there has been some debate as to whether type II fibers hypertrophy to a greater degree than type I fibers (16, 40). Therefore, the purpose of this study was to examine hypertrophic mechanisms in the plantaris and soleus muscles during the rapid hypertrophic growth phase (i.e., 14 days) following dual-overload surgery in rats. We hypothesized that the type II fiber-prominent plantaris muscle would hypertrophy more than the type I-prominent soleus muscle due to *1*) an enhanced ribosome biogenesis response in the overloaded plantaris muscle, *2*) an enhanced protein synthetic response in the overloaded plantaris muscle, *3*) an enhanced satellite cell proliferation response in the overloaded plantaris muscle, and/or *4*) a larger decrease in muscle proteasome activity in the plantaris muscle.

MATERIALS AND METHODS

Animal experimental procedures. All procedures were approved by the Auburn University Institutional Animal Care and Use Committee.

Address for reprint requests and other correspondence: M. D. Roberts, School of Kinesiology, Molecular and Applied Sciences Laboratory, Auburn University, 301 Wire Rd., Office 286, Auburn, AL 36849 (e-mail: mdr0024@auburn.edu).

Twelve Wistar rats (3 mo old; 6 female, 6 male) were purchased from Harlan Laboratories (Indianapolis, IN) and allowed to acclimate in a dedicated animal housing facility on the Auburn University campus for 2 wk before SA surgeries. Animal quarters were maintained on a constant 12:12-h light-dark cycle at ambient room temperature. Water and rodent chow (AIN-93G formula) were provided ad libitum during the 2-wk acclimation period as well as following surgeries.

On the morning of surgeries, rat cages were removed from the animal quarters and placed in an adjacent anteroom, where the surgeries occurred. Briefly, each rat was placed belly-down on a heating pad and anesthetized using vaporized isoflurane via oxygen delivery. For the dual-overloaded leg [right leg on each animal (SA)], an incision was made halfway up the leg, the distal portion of the gastrocnemius tendon was completely severed, approximately one-half of the distal portion of the gastrocnemius muscle was removed, and the incision was closed with sutures. Immediately following the SA leg procedure, a sham surgery (CTL) was performed on the left leg: a similar incision was made and sutured without gastrocnemius tendon modifications or muscle removal. Immediately following these procedures, ketoprofen (15 mg/kg ip) was injected, and the animals were placed in a recovery cage, where they were individually housed. While beam-break data were not collected, visual inspection indicated that activity levels of the animals returned to presurgical levels ~1–2 days after SA. Rats remained in their cages until they were euthanized 14 days following surgery. Surgical procedures averaged ~10 min per rat. Additionally, rats were weighed 1–3 days postsurgery to ensure that they were recovering properly; all rats adequately recovered following the surgical procedure.

On the morning of dissections (0600–0700, 14 days postsurgery), food was removed from home cages, resulting in a ~4-h fast. Animals were transported to the Auburn University School of Kinesiology and allowed to acclimate for 3–4 h. Before euthanasia (30 min), animals were injected with puromycin dihydrochloride (0.021 mg/g body mass ip diluted in 1 mL of PBS; catalog no. AAJ61278-MC, VWR International, Rando, PA) to determine relative protein synthesis levels via the SUnSET method (12). Thereafter, rats were euthanized under CO_2 gas in a 2-L induction chamber (VetEquip, Pleasanton, CA). During dissections, the soleus and plantaris muscles were rapidly extracted and weighed using an analytical scale with a sensitivity of 0.0001 g (Mettler-Toledo, Columbus, OH). Muscles were cut in very close proximity at the origin and insertion sites, and visible connective tissue at both ends was delicately removed with surgical scissors.

Approximately 50 mg of tissue from the midbelly of each muscle were placed in cryomolds containing freezing medium (catalog no. 4583, Tissue-Tek, Sakura Finetek, Torrance, CA). Cryomolds were frozen using liquid nitrogen-cooled isopentane and then stored at −80°C until immunofluorescent staining for fiber cross-sectional area (fCSA), myonuclear number, and satellite cell number. Approximately 30 mg of tissue from both muscles were then placed in 1.7-mL tubes containing 500 μL of ice-cold general cell lysis buffer [20 mM Tris·HCl (pH 7.5), 150 mM NaCl, 1 mM Na-EDTA, 1 mM EGTA, 1% Triton, 20 mM sodium pyrophosphate, 25 mM sodium fluoride, 1 mM β-glycerophosphate, 1 mM Na_3O_4, and 1 μg/mL leupeptin; catalog no. 9803, Cell Signaling Technology, Danvers, MA]. Samples were homogenized via micropestle manipulation, insoluble proteins were removed by centrifugation at 500 *g* for 5 min, and supernatants were stored at −80°C for immunoblot analysis. Approximately 30 mg of tissue from both muscles were placed in 1.7-mL tubes containing 500 μL of RiboZol (catalog no. N580, Amresco, Solon, OH). On the day of dissections, samples were homogenized by micropestle manipulation, and RNA was isolated according to the manufacturer's recommendations. Thereafter, RNA was frozen at −80°C until quantification using a spectrophotometer (NanoDrop Lite, Thermo Fisher Scientific, Waltham, MA). While values in the current study were not recorded, our laboratory has consistently obtained RNA yielding 260/280- and 260/230-nm ratio readings >1.90. Notably, one female rat yielded extraordinarily low RNA, so 11 rats were included in this analysis. Remaining tissue was placed in a prelabeled foil, flash-frozen in liquid nitrogen, and banked at −80°C.

Western blotting and 20S proteasome activity determination. Cell lysis buffer supernatants were assayed for soluble protein concentrations using the bicinchoninic acid assay (catalog no. 23225, Thermo Fisher Scientific). Tissue homogenates were prepared for Western blotting using 4× Laemmli buffer at 2 μg/μL. MPS levels were determined using the Western blot SUnSET method, as previously described by our laboratory (29, 30). An enhanced chemiluminescence reagent (catalog no.WBLUF0500, MilliporeSigma, Burlington, MA) was used for membrane development, and band densitometry was performed using a gel documentation system and associated densitometry software (UVP). All data were normalized to the CTL plantaris or soleus mean value and expressed as relative expression units. One female rat injected with puromycin dihydrochloride did not show a puromycin signal, so 11 rats were included in this analysis. The anti-puromycin antibody (catalog no. MABE342, MilliporeSigma) has been validated by our laboratory (26).

Assays of 20S proteasome activity on plantaris and soleus cell lysates were also performed using a commercially available fluorometric kit according to the manufacturer's instructions (catalog no. APT280, MilliporeSigma), as previously described by our laboratory (29, 30). All data are expressed as relative fluorescence units per 40 μg of input protein.

Histology for fCSA, myonuclear number, and satellite cell number. Histology for fCSA, myonuclear number, and satellite cell number was performed as previously described by our laboratory (28). Briefly, a cryotome (Leica Biosystems, Buffalo Grove, IL) was used to cut 10-μm-thick sections from optimal cutting temperature compound-preserved samples, and the sections were adhered to positively charged histology slides. Once all samples were sectioned, batches were processed for immunohistochemistry. During batch processing, sections were air-dried at room temperature for 10 min, permeabilized in a PBS solution containing 0.5% Triton X-100 for 5 min, and blocked with 100% commercial blocking reagent (catalog no. 37515, Thermo Fisher Scientific) for 25 min.

After they were blocked, the sections were incubated for 60 min with a prediluted commercially available primary antibody solution containing rabbit anti-dystrophin IgG (catalog no. PA5-32388, Thermo Fisher Scientific) and a 1:15 dilution of mouse anti-Pax7 IgG supernatant (catalog no. Pax7, Hybridoma Bank, Iowa City, IA). Sections were then washed three times for 5 min each in 1× PBS and incubated in darkness for 60 min with a secondary antibody solution containing a 1:100 dilution of Texas Red-conjugated anti-rabbit IgG (catalog no. TI-1000, Vector Laboratories) and Alexa Fluor 488-conjugated anti-mouse IgG (catalog no. A-11001, Thermo Fisher Scientific). Sections were then washed three times for 5 min each in 1× PBS, air-dried, and mounted with fluorescent medium containing DAPI (catalog no. 30920, GeneTex, Irvine, CA). Sections were mounted on slides, which were stored in darkness at 4°C until immunofluorescent images were obtained.

Sections were stained, and two digital images per sample were captured using a fluorescence microscope (Nikon Instruments, Melville, NY) and a ×20 objective. Approximate exposure times were 600 ms for red and green imaging and 30 ms for blue imaging. Our staining method allowed the identification of cell membranes (detected by the Texas Red filter), small green cell bodies as satellite cells (detected by the FITC filter), and myonuclei (detected by the DAPI filter). fCSA and myonuclear number per fiber were measured using the open-sourced software MyoVision, with a pixel conversion ratio of 0.493 to account for the size and bit depth of images (42). For myonuclear quantification, the software automatically assigns stained nuclei to corresponding muscle fibers, where nuclei within the dystrophin border are counted and those outside the border are not counted. Myonuclear domain sizes for individual fibers were then calculated by dividing a given fCSA by the number of nuclei assigned

to the fiber. A technician who was blinded to the treatments used a grid function in NIS Elements software (Nikon Instruments) and a hand-held tally counter to manually count satellite cells.

Plantaris dehydration methodology for assessing edema. Snap-frozen plantaris samples (~20 mg) were freeze-dried using a laboratory-grade freeze-drying device (FreeZone 2.5, Labconco, Kansas City, MO). The condenser was set at −50°C and the vacuum at 0.1 mbar, and samples were placed in the condenser well for 4 h under vacuum pressure. After freeze-drying was completed, muscle was reweighed on an analytical scale to determine fluid content. We only had enough plantaris tissue from nine rats and lacked soleus muscle to complete this analysis.

Statistics. A two-way ANOVA (soleus vs. plantaris muscle and CTL vs. SA leg) was used to analyze all dependent variables, except plantaris fluid content, without consideration of sex, and statistical significance was set at $P < 0.05$. When a significant main effect or interaction was obtained, least significant difference (LSD) post hoc tests were performed. Plantaris fluid content comparisons between SA and CTL legs were performed using a dependent-samples *t* test, and statistical significance was set at $P < 0.05$.

For the sex analysis, a three-way ANOVA (soleus vs. plantaris muscle, CTL vs. SA leg, and male vs. female) was used to analyze all dependent variables, and statistical significance was set at $P < 0.05$. Again, when a significant main effect or interaction was obtained, LSD post hoc tests were performed.

RESULTS

Plantaris and soleus masses. Body masses of the rats were as follows (means ± SD): 261 ± 19 g for males, 150 ± 8 g for females, and 206 ± 60 g for both sexes combined (data not shown). A main effect of surgery was evident for body weight-corrected muscle masses (CTL < SA, $P < 0.001$), as was a muscle × surgery interaction ($P < 0.001$; Fig. 1*A*). Post hoc analysis indicated greater soleus and plantaris mass in the SA than CTL leg ($P < 0.001$; Fig. 1*A*). A main effect of surgery was evident for absolute muscle mass (CTL < SA, $P = 0.008$), although a muscle × surgery interaction did not reach the threshold for significance ($P = 0.074$; Fig. 1*B*). Given the significant interaction for body weight-corrected muscle mass, we sought to determine the degree to which each SA muscle hypertrophied relative to the CTL muscle. Interestingly, in the SA leg, the degree of hypertrophy was significantly greater for the plantaris than soleus muscle (Fig. 1*C*).

Plantaris and soleus histology. A main effect of surgery was evident for fCSA (CTL < SA, $P = 0.026$; Fig. 2*A*). Post hoc analysis indicated greater values in the SA than CTL leg for the soleus ($P = 0.045$) and a trend toward significance for the plantaris muscle ($P = 0.054$). Main effects of muscle (plantaris < soleus, $P < 0.001$) and surgery (CTL < SA, $P = 0.008$) were evident for myonuclear number, as was a significant interaction ($P = 0.008$; Fig. 2*B*). Post hoc analysis indicated greater values in the SA than CTL leg for the soleus ($P = 0.008$), but not the plantaris ($P = 0.857$), muscle. Main effects of muscle (soleus < plantaris, $P < 0.001$) were evident for myonuclear domain size (Fig. 2*C*). Post hoc analysis indicated a tendency for greater values in the SA than CTL leg for the plantaris ($P = 0.052$), but not the soleus ($P = 0.184$), muscle. Main effects of muscle (soleus < plantaris, $P = 0.028$) and surgery (CTL < SA, $P = 0.048$) were evident for satellite cell number, as was a significant interaction ($P = 0.002$; Fig. 2*D*). Post hoc analysis indicated greater values in the SA than CTL leg for the plantaris ($P = 0.003$), but not the soleus ($P = 0.857$), muscle. Fiber counts for fCSA analyses were as follows (means ± SD): 139 ± 32 and 132 ± 28 for CTL and SA soleus, respectively, and 147 ± 41 and 134 ± 43 for CTL and SA plantaris, respectively. Fiber counts for satellite cell quantification were as follows (means ± SD): 245 ± 29 and 217 ± 30 for CTL and SA soleus, respectively, and 259 ± 39 and 230 ± 45 for CTL and SA plantaris, respectively.

Hypertrophic mechanisms in plantaris and soleus muscles. A main effect of surgery was evident for MPS levels (CTL < SA, $P = 0.029$; Fig. 3*A*). Post hoc analysis indicated greater MPS levels in the plantaris SA than CTL leg ($P = 0.038$), whereas levels were similar between soleus SA and CTL legs ($P = 0.254$). Main effects of muscle (soleus < plantaris, $P < 0.001$) and surgery were evident for 20S proteasome activity (SA < CTL, $P < 0.001$; Fig. 3*B*). Additionally, a muscle × surgery interaction existed ($P < 0.001$). Post hoc analysis indicated lower 20S proteasome activity levels in the SA than CTL leg for both muscles. However, downregulation of 20S proteasome activity was more robust in the SA than CTL leg in the plantaris than soleus muscle (−63% vs. −20%, $P = 0.001$). A main effect of muscle on total RNA concentrations was evident (plantaris < soleus, $P < 0.001$; Fig. 3*C*). Post hoc analysis indicated greater total RNA concentrations in the

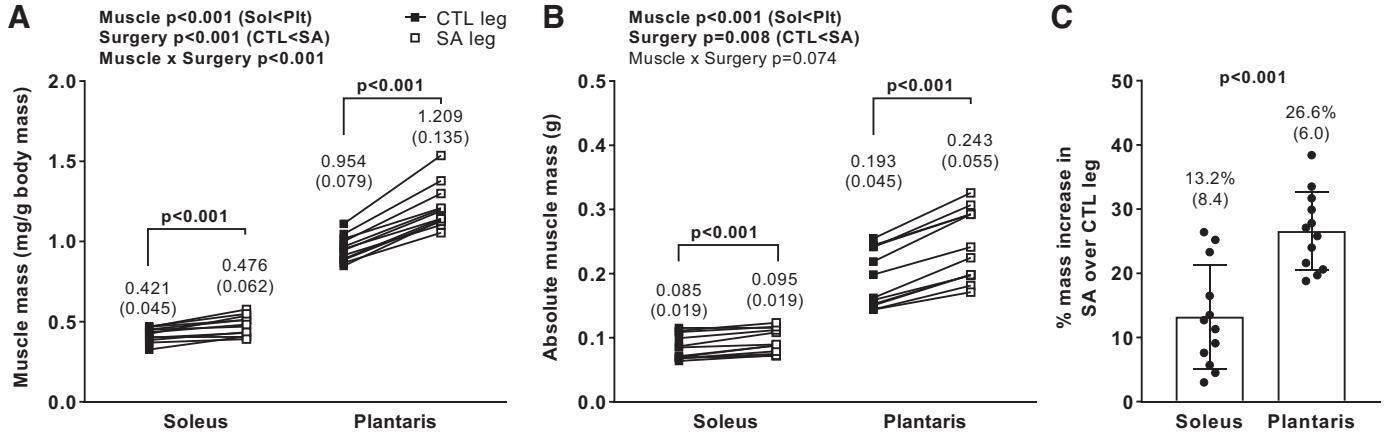

Fig. 1. Plantaris hypertrophy occurs to a greater degree following 14 days of dual overload. Body weight-corrected soleus (Sol) and plantaris (Plt) muscle mass (*A*) and absolute mass (*B*) data indicate that both muscles hypertrophied 14 days following unilateral dual-overload synergist ablation (SA). However, the type II-prominent plantaris muscle hypertrophied to a greater degree than the type I-prominent soleus muscle (*C*). Data are from 12 rats (6 male, 6 female) that were 4 mo of age at the time of euthanasia. Individual values are shown with means ± SD (in parentheses). CTL, sham/control leg.

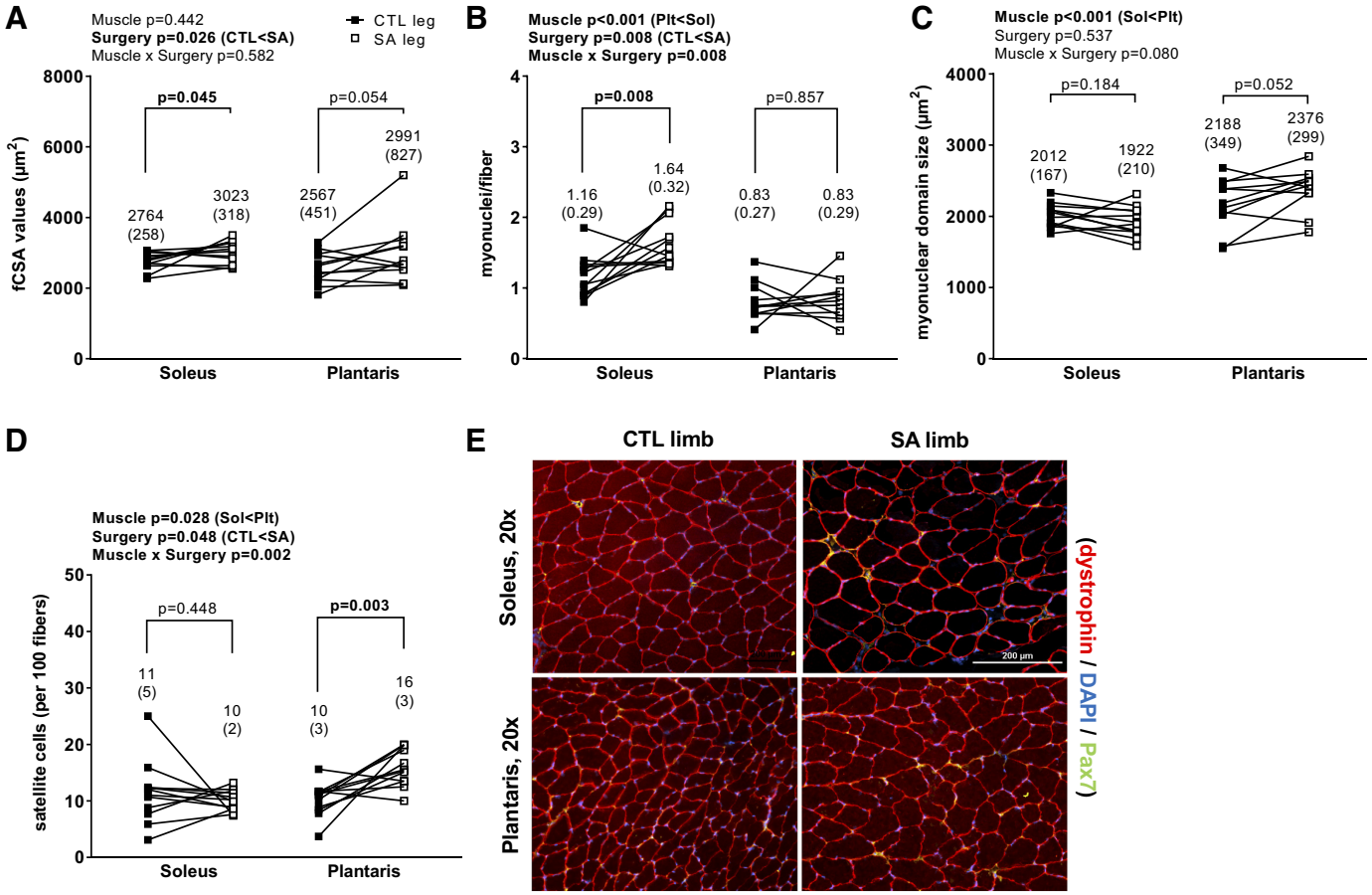

Fig. 2. Plantaris and soleus histology. Fiber cross-sectional area (fCSA) analysis indicates significant hypertrophy of soleus (Sol) muscles and a trend toward significance for plantaris (Plt) muscles 14 days following unilateral dual-overload synergist ablation [SA (*A*)]. However, only the SA soleus muscle exhibited myonuclear accretion (*B*), which led to preservation of the myonuclear domain in the SA soleus muscle but a tendency to an increase in the myonuclear domain in the SA plantaris muscle (*C*). Satellite cell number increased in the SA plantaris, but not in the SA soleus, muscle (*D*). Individual values are shown with means ± SD (in parentheses). *E*: representative ×20 histological images; scale bar = 200 μm. CTL, sham/control leg.

plantaris SA than CTL leg ($P = 0.013$), whereas levels were similar between soleus SA and CTL legs ($P = 0.869$). Main effects of muscle (soleus < plantaris, $P < 0.001$) and surgery were evident for estimated total RNA content (CTL < SA, $P = 0.001$; Fig. 3*D*). Additionally, a muscle × surgery interaction existed ($P = 0.017$). Post hoc analysis indicated an increase in estimated total RNA content in the SA compared with the CTL leg for the plantaris muscle ($P < 0.001$), whereas values were similar between soleus SA and CTL legs ($P = 0.105$). Our tissue fluid analysis on the plantaris muscle indicated that values were similar between SA and CTL legs ($P = 0.555$; Fig. 3*E*).

Soluble protein concentrations in plantaris and soleus muscles. Given that markers of ribosome biogenesis and protein turnover were more affected in SA plantaris than soleus muscles, we examined if soluble protein content differed between limbs. While a main effect of muscle was evident for soluble protein concentrations (soleus < plantaris, $P = 0.004$; Fig. 4*A*), neither a main effect of surgery nor an interaction was present. We mathematically estimated soluble protein content by multiplying concentrations by muscle masses. Again, a main effect of muscle was evident for soluble protein concentrations (soleus < plantaris, $P < 0.001$; Fig. 4*B*), although neither a main effect of surgery nor an interaction was present.

Sex differences. Female rats presented larger body weight-corrected muscle masses and lower absolute muscle masses (i.e., sex effects, $P < 0.001$; data not shown); however, no sex × surgery or sex × surgery × muscle interaction was evident for these variables. Female rats also presented less soluble protein content on a concentration and an estimated total basis (i.e., sex effects, $P < 0.001$; data not shown), as well as less estimated total RNA content; however, again, no sex × surgery or sex × surgery × muscle interaction was evident for these variables. Interestingly, there was a sex × surgery × muscle interaction for total RNA concentrations. Post hoc analyses indicated higher values in the SA than CTL plantaris of female rats (453 ± 36 vs. 342 ± 45 μg/mg wet mass, $P = 0.027$), whereas SA and CTL plantaris values were similar in male rats (388 ± 62 and 357 ± 57 μg/mg wet mass, respectively, $P = 0.243$; data not shown). No significant main effects of sex or sex-related interactions were evident for MPS levels, 20S proteasome activity levels, fCSA values, myonuclear number, myonuclear domain size, or satellite cell number.

DISCUSSION

The current study demonstrates that the type II fiber-prominent plantaris muscle hypertrophies to a greater extent than the

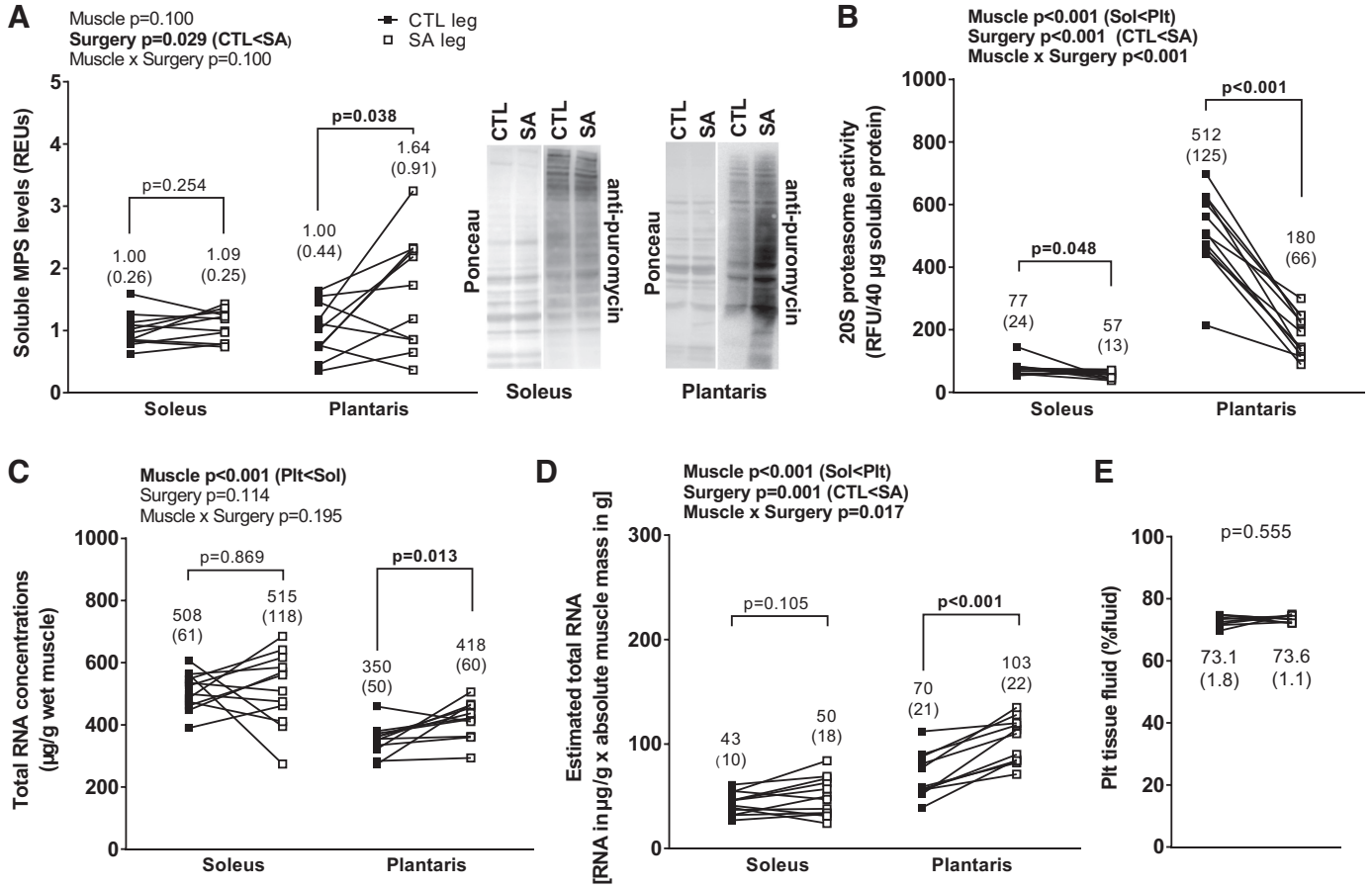

Fig. 3. Hypertrophic mechanisms in overloaded plantaris (Plt) and soleus (Sol) muscles. Data suggest increased muscle protein synthesis (MPS) levels (n = 11 rats, *A*) only in the plantaris muscle 14 days following unilateral dual-overload synergist ablation (SA). REUs, relative expression units. 20S proteasome activity (a surrogate of muscle proteolysis) decreased in the SA plantaris and soleus muscles (n = 12 rats; *B*), although the magnitude of the decrease was more robust in the plantaris muscle. Total RNA concentration and estimated total content (suggestive of ribosome biogenesis) increased in the SA plantaris muscle only (n = 11 rats for plantaris, n = 12 rats for soleus; *C* and *D*). Plantaris muscle fluid (determined by weight differential analysis after tissue dehydration) was not different between SA and CTL legs (n = 9 rats; *E*), indicating that edema did not contribute to tissue growth (we lacked adequate soleus muscle to perform this analysis). Individual values are shown with means ± SD (in parentheses). CTL, sham/control leg.

type I fiber-prominent soleus muscle during dual-overload SA. We also report that comprehensive biomarkers related to hypertrophy (MPS levels, ribosome density, satellite cell number, and 20S proteasome activity) were more favorably affected in the overloaded plantaris than soleus muscle. Our findings are summarized in Fig. 5.

Our histology data suggest similar fCSA increases in response to SA in fibers within each muscle group (plantaris SA/CTL = +17%, soleus SA/CTL = +9%, $P > 0.100$), despite the body weight-corrected muscle mass data indicating a greater degree of hypertrophy in the SA plantaris than the SA soleus (plantaris SA/CTL = +27%, soleus SA/CTL = +13%, $P < 0.001$). While these findings are difficult to reconcile, numerous animal studies comparing muscle mass with fCSA changes in response to overload stimuli report conflicting results (reviewed in Ref. 13). These inconsistencies are (in part) likely related to the fact that histology only enables the two-dimensional quantification of hundreds of muscle fibers, whereas assessment of intact muscle masses accounts for the three-dimensional characteristics of thousands of muscle fibers. In support of this contention, a recent letter to the editor by Jorgenson and Hornberger described nuances that occur during SA-induced plantaris hypertrophy (20). Specifically, they noted that the plantaris muscle can undergo significant changes in muscle pennation angle, as well as increases in fiber length (a variable that can increase muscle mass without affecting fCSA), neither of which is accounted for by histological analysis. It is also possible that hyperplasia may have contributed to discrepancies in the findings. Fiber splitting may have contributed to the lack of a significant increase in plantaris myonuclear number in the SA leg. However, fiber splitting has been inconsistently reported in compensatory hypertrophic models (1). Nevertheless, and as we previously posited (19), the assessment of intact/whole muscle mass provides a stronger basis for skeletal muscle hypertrophy than two-dimensional fCSA assessment.

Disagreement in the aforementioned data aside, our plantaris and soleus data agree with numerous prior studies. DeVol et al. (7) reported superior plantaris hypertrophy compared with soleus hypertrophy after 8 days of unilateral dual overload, and similar results were reported by Thomson and Gordon (39). Contrary to the current data, however, neither study extensively examined the hypertrophic mechanisms involved. Chalé-Rush et al. (4) similarly reported that plantaris hyper-

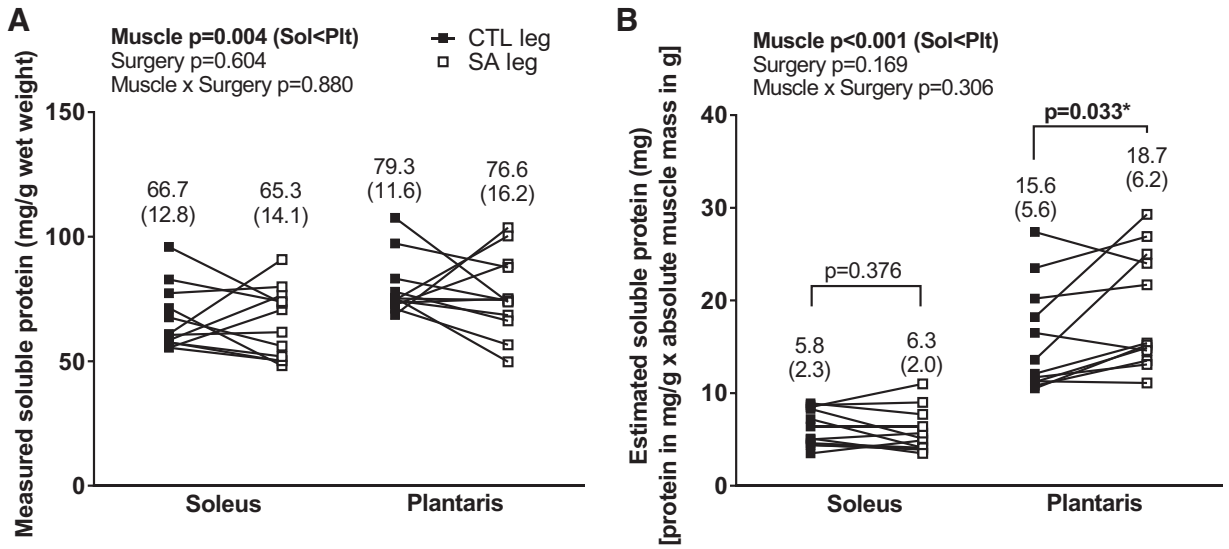

Fig. 4. Soluble protein content of plantaris (Plt) and soleus (Sol) muscles (n = 12 rats; *A*) and estimated soluble protein per muscle (n = 12; *B*). While there were only main effects of muscle for each variable, data in *B* illustrate greater estimated soluble protein in plantaris muscle 14 days following dual-overload synergist ablation (SA) than in the control (CTL) leg, whereas values were similar in soleus SA and CTL legs. ["Forced" post hoc test was performed (for discussion purposes only) due to lack of an interaction.] Individual values are shown with means ± SD (in parentheses).

trophy occurs to a greater extent than soleus hypertrophy in 6- and 30-mo old rats after 28 days of dual overload. Additionally, they reported elevated phosphorylation of proteins related to translation initiation [e.g., mechanistic target of rapamycin (mTOR) and ribosomal protein S6] in the overloaded (SA), but not CTL, plantaris muscle at this time point. These data agree with our current data suggesting that MPS levels were only elevated in the plantaris SA muscle 14 days following dual overload and, more broadly, that type II fibers may exhibit a heightened and/or prolonged protein synthetic response to a compensatory overload stimulus relative to type I fibers. In support of this hypothesis, Gordon et al. (14) reported that the

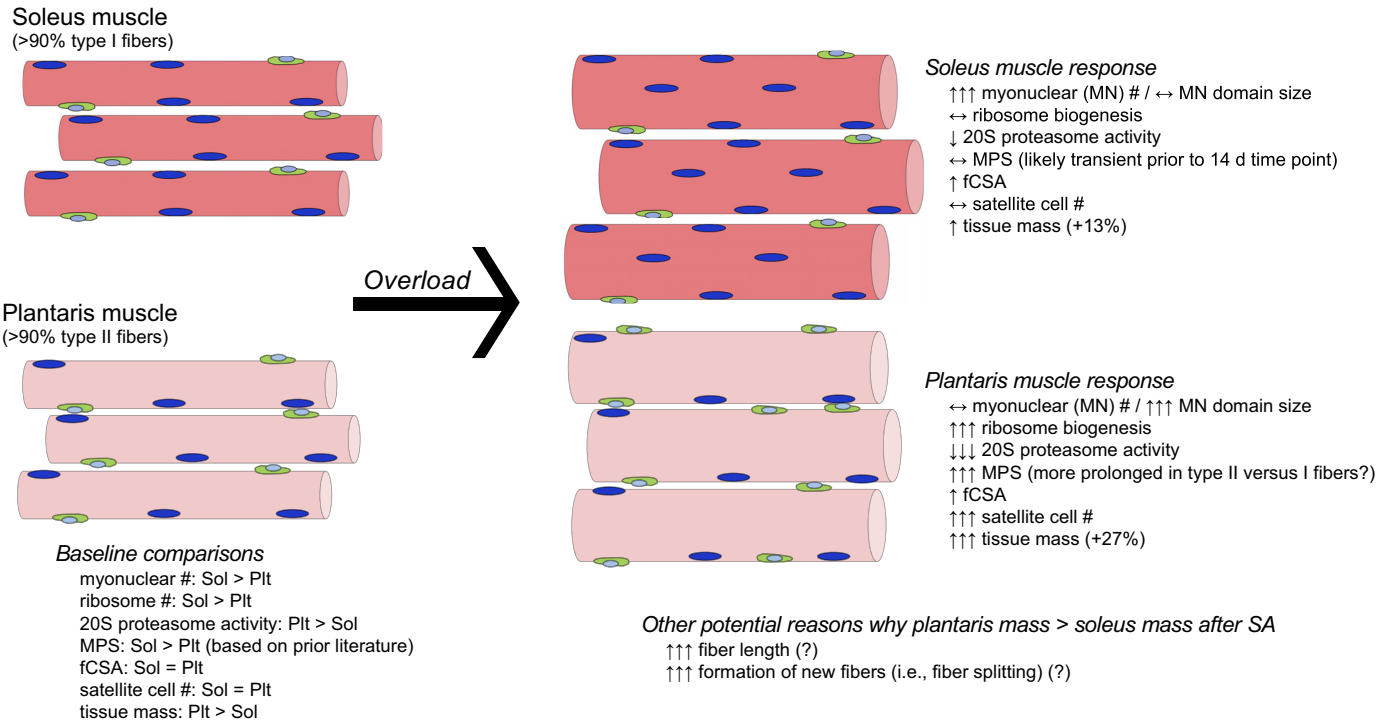

Fig. 5. Soleus (Sol) and plantaris (Plt) muscle characteristics before (*left*) and 14 days following (*right*) dual-overload synergist ablation (SA). We also speculate on other (unmeasured) variables that might explain why the type II fiber-prominent plantaris muscle hypertrophied more than the soleus muscle following SA. ↔, no change with overload; ↑, Significant increase in SA compared with CTL leg; ↑ ↑ ↑, significant increase in SA compared with CTL leg, as well as a greater-magnitude increase in SA plantaris or soleus than the other muscle; ↓, significant decrease in SA compared with CTL leg; ↓ ↓ ↓, significant decrease in SA compared with CTL leg, as well as a greater-magnitude decrease in SA plantaris than soleus muscle. fCSA, fiber cross-sectional area.

phosphorylation of the focal adhesion kinase protein, which is involved in the mechanical activation of mTOR complex 1 signaling and muscle protein synthesis (15), was upregulated in overloaded soleus muscle 1 and 8 days following dual overload, whereas plantaris levels showed a more delayed increase that, conceivably, would have extended past 8 days of overload had the authors made these measurements. Our current data (Fig. 4*B*) also suggest accretion of estimated protein in the SA vs. CTL plantaris, whereas values were similar between legs in the soleus. While these data support the MPS findings between muscle groups, we use caution in interpreting this finding, given that we implemented a forced post hoc test to determine these differences. Collectively, these data suggest the possibility that the soleus muscle demonstrates a relatively rapid increase in MPS following compensatory overload, whereas the plantaris muscle may exhibit a heightened response that is significantly more prolonged. While the mechanistic underpinnings of these findings are difficult to ascertain, one possibility may be related to muscle recruitment patterns. Given that the soleus is a postural muscle likely recruited to a much greater extent than the plantaris in the nonoverload state (6), soleus muscle mass may have already reached a growth plateau relative to the plantaris muscle before overload. Additionally, it is likely that the increase in muscle fiber activation is greater in the plantaris than soleus following overload, which, again, may have been chiefly responsible for promoting more robust adaptations in the former muscle group. Indeed, these hypotheses support data suggesting that the soleus muscle tends to rapidly atrophy in rodents during unloading conditions relative to the plantaris muscle (37).

Beyond the aforementioned findings related to fiber type differences in MPS in response to overload, we report other notable results. Our sex analysis indicated that SA-induced ribosome biogenesis was seemingly elevated in female rats, whereas this response did not occur in male rats. It should be noted that our sex analysis was limited, in that only five or six rats of each sex were analyzed. Likewise, there is ample evidence in humans to suggest that males are capable of experiencing increases in ribosome biogenesis in response to resistance training (8, 18, 27, 34). Nevertheless, this observation does warrant further examination into whether overload-induced alterations in ribosome biogenesis are differentially regulated between sexes. The greater downregulation of SA plantaris than SA soleus 20S proteasome activity is also an intriguing finding. Classic studies, many of which were performed in the laboratories of Booth and Baldwin (36–38), indicate that hindlimb unloading preferentially promotes myofibrillar protein degradation in the soleus vs. plantaris muscle. While the overload model starkly contrasts with hindlimb unloading, our data suggest that proteolytic mechanisms in type II fibers may be more favorably adaptable in response to overload, and, again, this warrants future research consideration, as it relates to fiber type mechanistic differences. Although satellite cell number increased in response to overload in the plantaris, but not soleus, muscle, only the SA soleus muscle experienced an increase in myonuclear accretion. These data agree, in principle, with prior animal and human literature suggesting that *1*) type I fibers contain more myonuclei (and ribosomes) per fiber than type II fibers (17, 25) and *2*) during hypertrophy, the size of the myonuclear domain is tightly regulated in type I fibers, whereas the domain size increases in type II fibers without myonuclear accretion (10). Again, these data provided by the currently utilized model offer intriguing insight into mechanistic fiber type differences that occur in response to overload, and future studies implementing a time-course experiment with similar outcomes can provide more intricate details.

The primary motivation for performing studies such as the current investigation is to relate findings to the human condition. Indeed, others have made compelling arguments that the SA model provides a unique glimpse into how skeletal muscle adapts to a significant overload stressor (5, 23, 35). While it is difficult (if not impossible) to assess whether dual overload mimics exercise training, it is inviting to speculate how the dual-overload model relates to human resistance training, given that *1*) the model allows for comparison of type I fiber-with type II fiber-prominent muscle groups, and both fiber types adapt to training (9), *2*) the hypertrophy (+13% soleus and +27% plantaris) is similar to hypertrophy that could be achieved with weeks of resistance training in some individuals (32), and *3*) such hypertrophy is not nearly as extreme as in the plantaris-only-overload model in rodents, which can elicit a 40–120% increase in muscle mass over a 14-day period (35). In a recent commentary, Grgic and Schoenfeld (16) suggested that high-load resistance training may induce the preferential growth of type II vs. type I muscle fibers. While their suggestion is insightful, the overall lack of data in the literature precluded a discussion of the potential fiber type-specific mechanisms responsible for these outcomes. We recently examined type I and II fCSA changes in >70 previously untrained college-aged men who performed 12 wk of higher-load full-body resistance training (3 days/wk) (27). Although both fiber types in the vastus lateralis (on average) significantly hypertrophied, a comparative analysis of the degree of hypertrophy between type I and type IIa/x fibers was not reported. In agreement with the commentary by Grgic and Schoenfeld, a post hoc examination of these human data revealed 9.5% hypertrophy (on average) of type I fibers and 16.3% hypertrophy of type IIa/x fibers ($P < 0.05$ between fiber types). The current rodent data are in agreement with the contention of Grgic and Schoenfeld, as well as our aforementioned human data, that higher-intensity overload via resistance training elicits superior increases in type II fiber hypertrophy. Others have also reported that one bout of resistance exercise (3), as well as months of resistance training (41), increases only type II fiber satellite cell number in humans, which, again, agrees with the current rodent data, in that overload only increased plantaris satellite cell number. Therefore, while it is challenging to relate rodent data to human findings, particularly considering the inherent differences in the respective models employed (SA and resistance training, respectively), these current animal data seem to agree well with previously published human research suggesting more robust molecular adaptations in response to overload in the form of resistance training in type II fibers. Furthermore, we contend that the dual-overload model may have utility in examining fiber type adaptations in response to an overload stimulus that may partially mimic the overload stress induced in human skeletal muscle during periods of high-load resistance training.

Experimental considerations. While these data provide compelling evidence of more robust adaptations to overload in the type II fiber-dominant plantaris muscle than the soleus muscle,

certain limitations should be noted. *1*) As mentioned above, the overload model elicits a supraphysiological hypertrophic response that is not encountered with resistance training in humans. Thus, our data should be viewed with this limitation in mind. *2*) The manner in which we normalized our MPS data precluded comparison of levels between muscle groups; specifically, given that multiple Western blots were required to accommodate all samples, we were limited in performing plantaris analysis separately from soleus analysis. This is a critical point, because our data insinuate that the SA plantaris exhibits the most heightened MPS levels, whereas it is likely that MPS levels were greater in the soleus than the plantaris (regardless of overload), given that various reports have suggested greater rates of protein synthesis in type I muscle fibers in animals (21, 24). *3*) While we were adequately powered with *n* sizes of 11–12 animals to detect SA vs. CTL leg differences in several variables, we were likely underpowered to detect small changes in other variables (e.g., fCSA) between legs.

Perspectives and Significance

These data replicate prior findings by clearly demonstrating hypertrophy to a greater extent in the type II-prominent plantaris than the type I-prominent soleus muscle in response to overload in rats. This study expands on these findings, suggesting that this response coincides with superior increases in MPS levels, ribosome biogenesis, and satellite cell proliferation and superior decreases in 20S proteasome activity in the overloaded plantaris compared with soleus muscle. These responses seem to be minimally influenced by sex, although differential stimulation of ribosome biogenesis via SA in the plantaris muscle warrants further investigation. Given that many findings from this study agree, in principle, with various human resistance-training experiments, we posit that the dual-overload model holds exciting promise to further delineate type I vs. type II fiber hypertrophic mechanisms that may be translatable to humans.

GRANTS

This study was funded by an internal Auburn University grant awarded to A. N. Kavazis, M. D. Roberts, and K. C. Young.

DISCLOSURES

No conflicts of interest, financial or otherwise, are declared by the authors.

AUTHOR CONTRIBUTIONS

M.D.R. and A.N.K. conceived and designed research; M.D.R. and C.B.M. performed experiments; M.D.R. and C.T.H. analyzed data; M.D.R., C.G.V., C.T.H., B.J.S., K.C.Y., and A.N.K. interpreted results of experiments; M.D.R. and C.B.M. prepared figures; M.D.R. drafted manuscript; M.D.R., C.B.M., C.G.V., C.T.H., B.J.S., K.C.Y., and A.N.K. edited and revised manuscript; M.D.R., C.B.M., C.G.V., C.T.H., B.J.S., K.C.Y., and A.N.K. approved final version of manuscript.

REFERENCES

1. **Antonio J, Gonyea WJ.** Skeletal muscle fiber hyperplasia. *Med Sci Sports Exerc* 25: 1333–1345, 1993. doi:10.1249/00005768-199312000-00004.
2. **Carlson CJ, Booth FW, Gordon SE.** Skeletal muscle myostatin mRNA expression is fiber-type specific and increases during hindlimb unloading. *Am J Physiol Regul Integr Comp Physiol* 277: R601–R606, 1999. doi:10.1152/ajpregu.1999.277.2.R601.
3. **Cermak NM, Snijders T, McKay BR, Parise G, Verdijk LB, Tarnopolsky MA, Gibala MJ, Van Loon LJ.** Eccentric exercise increases satellite cell content in type II muscle fibers. *Med Sci Sports Exerc* 45: 230–237, 2013. doi:10.1249/MSS.0b013e318272cf47.
4. **Chalé-Rush A, Morris EP, Kendall TL, Brooks NE, Fielding RA.** Effects of chronic overload on muscle hypertrophy and mTOR signaling in young adult and aged rats. *J Gerontol A Biol Sci Med Sci* 64A: 1232–1239, 2009. doi:10.1093/gerona/glp146.
5. **Cholewa J, Guimarães-Ferreira L, da Silva Teixeira T, Naimo MA, Zhi X, de Sá RB, Lodetti A, Cardozo MQ, Zanchi NE.** Basic models modeling resistance training: an update for basic scientists interested in study skeletal muscle hypertrophy. *J Cell Physiol* 229: 1148–1156, 2014. doi:10.1002/jcp.24542.
6. **Deschenes MR, Gaertner JR, O'Reilly S.** The effects of sarcopenia on muscles with different recruitment patterns and myofiber profiles. *Curr Aging Sci* 6: 266–272, 2013. doi:10.2174/18746098113066660035.
7. **DeVol DL, Rotwein P, Sadow JL, Novakofski J, Bechtel PJ.** Activation of insulin-like growth factor gene expression during work-induced skeletal muscle growth. *Am J Physiol Endocrinol Metab* 259: E89–E95, 1990. doi:10.1152/ajpendo.1990.259.1.E89.
8. **Figueiredo VC, Caldow MK, Massie V, Markworth JF, Cameron-Smith D, Blazevich AJ.** Ribosome biogenesis adaptation in resistance training-induced human skeletal muscle hypertrophy. *Am J Physiol Endocrinol Metab* 309: E72–E83, 2015. doi:10.1152/ajpendo.00050.2015.
9. **Fry AC.** The role of resistance exercise intensity on muscle fibre adaptations. *Sports Med* 34: 663–679, 2004. doi:10.2165/00007256-200434100-00004.
10. **Fry CS, Noehren B, Mula J, Ubele MF, Westgate PM, Kern PA, Peterson CA.** Fibre type-specific satellite cell response to aerobic training in sedentary adults. *J Physiol* 592: 2625–2635, 2014. doi:10.1113/jphysiol.2014.271288.
11. **Goldberg AL.** Work-induced growth of skeletal muscle in normal and hypophysectomized rats. *Am J Physiol* 213: 1193–1198, 1967. doi:10.1152/ajplegacy.1967.213.5.1193.
12. **Goodman CA, Hornberger TA.** Measuring protein synthesis with SUnSET: a valid alternative to traditional techniques? *Exerc Sport Sci Rev* 41: 107–115, 2013. doi:10.1097/JES.0b013e3182798a95.
13. **Gordon EE.** Anatomical and biochemical adaptations of muscle to different exercises. *JAMA* 201: 755–758, 1967. doi:10.1001/jama.1967.03130100053013.
14. **Gordon SE, Flück M, Booth FW.** Skeletal muscle focal adhesion kinase, paxillin, and serum response factor are loading dependent. *J Appl Physiol (1985)* 90: 1174–1183, 2001. doi:10.1152/jappl.2001.90.3.1174.
15. **Graham ZA, Gallagher PM, Cardozo CP.** Focal adhesion kinase and its role in skeletal muscle. *J Muscle Res Cell Motil* 36: 305–315, 2015. doi:10.1007/s10974-015-9415-3.
16. **Grgic J, Schoenfeld BJ.** Are the hypertrophic adaptations to high and low-load resistance training muscle fiber type specific? *Front Physiol* 9: 402, 2018. doi:10.3389/fphys.2018.00402.
17. **Habets PE, Franco D, Ruijter JM, Sargeant AJ, Pereira JA, Moorman AF.** RNA content differs in slow and fast muscle fibers: implications for interpretation of changes in muscle gene expression. *J Histochem Cytochem* 47: 995–1004, 1999. doi:10.1177/002215549904700803.
18. **Haun CT, Vann CG, Osburn SC, Mumford PW, Roberson PA, Romero MA, Fox CD, Johnson CA, Parry HA, Kavazis AN, Moon JR, Badisa VLD, Mwashote BM, Ibeanusi V, Young KC, Roberts MD.** Muscle fiber hypertrophy in response to 6 weeks of high-volume resistance training in trained young men is largely attributed to sarcoplasmic hypertrophy. *PLoS One* 14: e0215267, 2019. doi:10.1371/journal.pone.0215267.
19. **Haun CT, Vann CG, Roberts BM, Vigotsky AD, Schoenfeld BJ, Roberts MD.** A critical evaluation of the biological construct skeletal muscle hypertrophy: size matters but so does the measurement. *Front Physiol* 10: 247, 2019. doi:10.3389/fphys.2019.00247.
20. **Jorgenson KW, Hornberger TA.** The overlooked role of fiber length in mechanical load-induced growth of skeletal muscle. *Exerc Sport Sci Rev* 47: 258–259, 2019. doi:10.1249/JES.0000000000000198.
21. **Kelly FJ, Lewis SE, Anderson P, Goldspink DF.** Pre- and postnatal growth and protein turnover in four muscles of the rat. *Muscle Nerve* 7: 235–242, 1984. doi:10.1002/mus.880070309.
22. **Kilikevicius A, Bunger L, Lionikas A.** Baseline muscle mass is a poor predictor of functional overload-induced gain in the mouse model. *Front Physiol* 7: 534, 2016. doi:10.3389/fphys.2016.00534.
23. **Kirby TJ, McCarthy JJ, Peterson CA, Fry CS.** Synergist ablation as a rodent model to study satellite cell dynamics in adult skeletal muscle. *Methods Mol Biol* 1460: 43–52, 2016. doi:10.1007/978-1-4939-3810-0_4.

24. **Laurent GJ, Sparrow MP, Bates PC, Millward DJ.** Turnover of muscle protein in the fowl (*Gallus domesticus*). Rates of protein synthesis in fast and slow skeletal, cardiac and smooth muscle of the adult fowl. *Biochem J* 176: 393–401, 1978. doi:10.1042/bj1760393.
25. **Liu JX, Höglund AS, Karlsson P, Lindblad J, Qaisar R, Aare S, Bengtsson E, Larsson L.** Myonuclear domain size and myosin isoform expression in muscle fibres from mammals representing a 100,000-fold difference in body size. *Exp Physiol* 94: 117–129, 2009. doi:10.1113/expphysiol.2008.043877.
26. **Mobley CB, Fox CD, Ferguson BS, Pascoe CA, Healy JC, McAdam JS, Lockwood CM, Roberts MD.** Effects of protein type and composition on postprandial markers of skeletal muscle anabolism, adipose tissue lipolysis, and hypothalamic gene expression. *J Int Soc Sports Nutr* 12: 14, 2015. doi:10.1186/s12970-015-0076-9.
27. **Mobley CB, Haun CT, Roberson PA, Mumford PW, Kephart WC, Romero MA, Osburn SC, Vann CG, Young KC, Beck DT, Martin JS, Lockwood CM, Roberts MD.** Biomarkers associated with low, moderate, and high vastus lateralis muscle hypertrophy following 12 weeks of resistance training. *PLoS One* 13: e0195203, 2018. doi:10.1371/journal.pone.0195203.
28. **Mobley CB, Haun CT, Roberson PA, Mumford PW, Romero MA, Kephart WC, Anderson RG, Vann CG, Osburn SC, Pledge CD, Martin JS, Young KC, Goodlett MD, Pascoe DD, Lockwood CM, Roberts MD.** Effects of whey, soy or leucine supplementation with 12 weeks of resistance training on strength, body composition, and skeletal muscle and adipose tissue histological attributes in college-aged males. *Nutrients* 9: 972, 2017. doi:10.3390/nu9090972.
29. **Mobley CB, Holland AM, Kephart WC, Mumford PW, Lowery RP, Kavazis AN, Wilson JM, Roberts MD.** Progressive resistance-loaded voluntary wheel running increases hypertrophy and differentially affects muscle protein synthesis, ribosome biogenesis, and proteolytic markers in rat muscle. *J Anim Physiol Anim Nutr (Berl)* 102: 317–329, 2018. doi:10.1111/jpn.12691.
30. **Mobley CB, Mumford PW, Kephart WC, Haun CT, Holland AM, Beck DT, Martin JS, Young KC, Anderson RG, Patel RK, Langston GL, Lowery RP, Wilson JM, Roberts MD.** Aging in rats differentially affects markers of transcriptional and translational capacity in soleus and plantaris muscle. *Front Physiol* 8: 518, 2017. doi:10.3389/fphys.2017.00518.
31. **Nakada S, Ogasawara R, Kawada S, Maekawa T, Ishii N.** Correlation between ribosome biogenesis and the magnitude of hypertrophy in overloaded skeletal muscle. *PLoS One* 11: e0147284, 2016. doi:10.1371/journal.pone.0147284.
32. **Roberts MD, Haun CT, Mobley CB, Mumford PW, Romero MA, Roberson PA, Vann CG, McCarthy JJ.** Physiological differences between low versus high skeletal muscle hypertrophic responders to resistance exercise training: current perspectives and future research directions. *Front Physiol* 9: 834, 2018. doi:10.3389/fphys.2018.00834.
33. **Schiaffino S, Dyar KA, Ciciliot S, Blaauw B, Sandri M.** Mechanisms regulating skeletal muscle growth and atrophy. *FEBS J* 280: 4294–4314, 2013. doi:10.1111/febs.12253.
34. **Stec MJ, Kelly NA, Many GM, Windham ST, Tuggle SC, Bamman MM.** Ribosome biogenesis may augment resistance training-induced myofiber hypertrophy and is required for myotube growth in vitro. *Am J Physiol Endocrinol Metab* 310: E652–E661, 2016. doi:10.1152/ajpendo.00486.2015.
35. **Terena SM, Fernandes KP, Bussadori SK, Deana AM, Mesquita-Ferrari RA.** Systematic review of the synergist muscle ablation model for compensatory hypertrophy. *Rev Assoc Med Bras (1992)* 63: 164–172, 2017. doi:10.1590/1806-9282.63.02.164.
36. **Thomason DB, Biggs RB, Booth FW.** Protein metabolism and β-myosin heavy-chain mRNA in unweighted soleus muscle. *Am J Physiol Regul Integr Comp Physiol* 257: R300–R305, 1989. doi:10.1152/ajpregu.1989.257.2.R300.
37. **Thomason DB, Booth FW.** Atrophy of the soleus muscle by hindlimb unweighting. *J Appl Physiol (1985)* 68: 1–12, 1990. doi:10.1152/jappl.1990.68.1.1.
38. **Thomason DB, Herrick RE, Surdyka D, Baldwin KM.** Time course of soleus muscle myosin expression during hindlimb suspension and recovery. *J Appl Physiol (1985)* 63: 130–137, 1987. doi:10.1152/jappl.1987.63.1.130.
39. **Thomson DM, Gordon SE.** Diminished overload-induced hypertrophy in aged fast-twitch skeletal muscle is associated with AMPK hyperphosphorylation. *J Appl Physiol (1985)* 98: 557–564, 2005. doi:10.1152/japplphysiol.00811.2004.
40. **van Wessel T, de Haan A, van der Laarse WJ, Jaspers RT.** The muscle fiber type-fiber size paradox: hypertrophy or oxidative metabolism? *Eur J Appl Physiol* 110: 665–694, 2010. doi:10.1007/s00421-010-1545-0.
41. **Verdijk LB, Gleeson BG, Jonkers RA, Meijer K, Savelberg HH, Dendale P, van Loon LJ.** Skeletal muscle hypertrophy following resistance training is accompanied by a fiber type-specific increase in satellite cell content in elderly men. *J Gerontol A Biol Sci Med Sci* 64A: 332–339, 2009. doi:10.1093/gerona/gln050.
42. **Wen Y, Murach KA, Vechetti IJ Jr, Fry CS, Vickery C, Peterson CA, McCarthy JJ, Campbell KS.** MyoVision: software for automated high-content analysis of skeletal muscle immunohistochemistry. *J Appl Physiol (1985)* 124: 40–51, 2018. doi:10.1152/japplphysiol.00762.2017.